American Journal of Electrical and Computer Engineering
2022; 6(2): 61-67
http://www.sciencepublishinggroup.com/j/ajece
doi: 10.11648/j.ajece.20220602.12
ISSN: 2640-0480 (Print); ISSN: 2640-0502 (Online)

A Novel Grid Corrosion Detection and Two-Dimensional Imaging Approach for a Grounding Substation

Mingyang Li[1, *], Shaorong Cao[1], Wei Niu[2], Mingdong Zhang[1], Weidong Xie[1]

[1]State Grid Gansu Electric Power Company, Lanzhou, China

[2]State Grid Gansu Electric Power Company Qiangyang Power Supply Company, Lanzhou, China

Email address:
limingyang202109@163.com (Mingyang Li)

[*]Corresponding author

To cite this article:
Mingyang Li, Shaorong Cao, Wei Niu, Mingdong Zhang, Weidong Xie. A Novel Grid Corrosion Detection and Two-Dimensional Imaging Approach for a Grounding Substation. *American Journal of Electrical and Computer Engineering*. Vol. 6, No. 2, 2022, pp. 61-67. doi: 10.11648/j.ajece.20220602.12

Received: June 29, 2022; **Accepted**: July 12, 2022; **Published**: July 28, 2022

Abstract: The grounding grid is one of the most important components of the power grid. However, the grounding grid is buried in the ground all year round, corrosion occurs commonly, which not only deteriorates the operation of the power system, but also could result in severe economic loss. The deterioration could be caused by the following reasons: the corrosion of metal conductors in the soil as time goes, the inevitable negligence or omission during construction (such as false welding, missing welding), and the electrodynamic effect of the ground current on the voltage equalizing conductor, etc. Since a well-performed grounding is essential for the security, cost-efficiency, and stability of the substation, the detection of grounding grid corrosion is necessary. In this paper, a new method for detecting the corrosion of the grounding grid is proposed. Specifically, this novel algorithm integrates the advantages of particle swarm optimization and least-squares method-particle swarm optimization. Also, it uses the least-squares algorithm for local tuning. We simulate three different corrosion situations – multiple branches, ring-shaped branches, and straight-lined branches. These simulation results show that our approach provides a very efficient and useful solution. More importantly, a real-world case study is implemented. The results of case study are consistent with the simulation results. Hence, this paper validates the effectiveness of the proposed algorithm on both simulation and experimental level.

Keywords: Grounding Substation, Grid Corrosion, Corrosion Detection, Corrosion Simulation

1. Introduction

Working grounding, lightning protection grounding, and protective grounding are the core part of the electrical equipment in the substation, which undertakes the important tasks of substation grounding networks [1, 2]. Often when the grounding short-circuits current of the power system gets bigger, the requirement of grounding reliability also becomes higher [5]. However, the grounding grid is buried in the ground all year round, corrosion occurs unavoidably, leading to a deterioration in grounding performance [10]. Apparently, the corrosion could be a threat to the stable operation of the power system. Therefore, based on the characterization parameters of the grounding grid, how to make accurate, reliable, and effective detections on the operating conditions and fault conditions of the grounding grid has become an important task in the field of electrical equipment detection and fault diagnosis [4, 7]. In other words, the engineering practical significance and economic benefits of grid operating detections are significant [8].

In power systems, the earth is commonly applied as a reference point, also known as a zero potential [9, 11]. The grounding is to connect a part of the electrical system or equipment tightly with the earth through a grounding device so that the conductor potential of this part is always maintained at the earth potential. The substation consists of important electrical equipment, such as transformers, arresters, and circuit breakers.

A well-performed grounding is essential for the security, cost-efficiency, and stability of the substation [12]. Based on their functions, the grounding techniques of substations can generally be categorized into the following three types: Work grounding (a. k. a., system grounding), Protective grounding, and Lightning protection grounding.

Since the grounding grid is buried in the ground all the time, the corrosion-resistant material has to be adopted. However, in some regions of China, due to the constraints of economic and resources, the galvanized carbon steel instead of copper is commonly used [3, 6]. Specifically, during the construction period of the substation, the horizontal pressure conductor made of galvanized flat steel or angle steel is welded to form a grounding grid and eventually buried in the ground [13, 14]. However, the performance of the grounding grid deteriorates, which could lead to the dysfunction of the ground flow of the short-circuit fault currents [15]. The deterioration could be caused by the following reasons: the corrosion of metal conductors in the soil as time goes, the inevitable negligence or omission during construction (such as false welding, missing welding), and the electrodynamic effect of the ground current on the voltage equalizing conductor, etc. It is noted worthy that soil corrosion is the most significant cause [16]. Especially in some saline-alkali soils, the corrosion of metal conductors could be very detrimental.

Hence, in this paper, we proposed a novel algorithm to detect the corrosion of the grounding grid. We simulate three different corrosion situations – multiple branches, ring-shaped branches, and straight-lined branches. These simulation results show that our approach provides a very efficient and useful solution.

2. Methodology

2.1. Corrosion Diagnosis Model of Substation Grounding Grid

The grounding grid is composed of various horizontal pressure conductors. Compared with the resistivity of the grounding grid material, the resistivity of soil is much larger. Given the above-mentioned condition, ignoring the influence of other factors in the soil, the grounding grid can be regarded as a pure resistance grid. The grounding grid is connected to the equipment through the grounding lead (i.e., the reachable node), thus the entire grounding grid can be converted into a multi-port grid. Then, the diagram is obtained by extracting the "m" reachable nodes in the grid, shown in Figure 1.

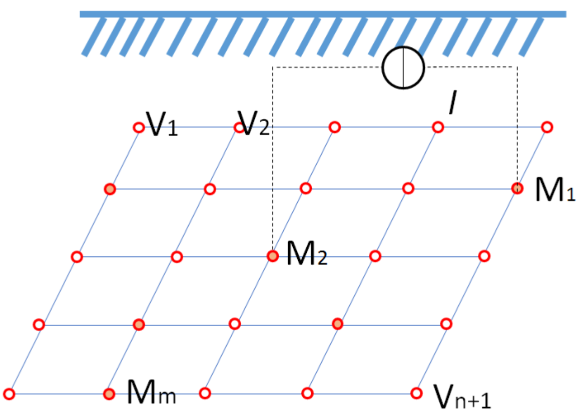

Figure 1. *Our proposed resistance network model for the grounding system.*

After the grounding grid is implemented, the resistivity, length, and cross-sectional area of each section of the conductor material are determined. The corresponding resistance value of each section of the conductor can be calculated by the resistance equation. After the grounding grid has been in operation for several years, multiple reasons may cause corrosion or even crack of the grounding grid. At this time, the resistance value of each branch could increase compared to the design value. Hence, only by applying the same excitation to the two resistances before and after the fault, and comparing the grounding resistance of the measurable node with the nominal value, the corrosion state of the grounding grid can be detected.

2.2. Our Proposed Algorithm

The conventional optimization algorithm often selects an initial value and then searches a path based on the algorithm's search strategy. Obviously, the search path is determined, hence only local extreme points can be obtained, rather than the global optimal solution. Given the characteristics of the grounding grid, the mathematical model of fault diagnosis is not a convex programming issue. Differently, the random search algorithm selects the initial value of the iteration randomly and the entire space can be applied to look for the global optimal solution. This paper proposes a novel algorithm that integrates the advantages of particle swarm optimization and least-squares method-particle swarm optimization that uses the least-squares algorithm for local tuning.

2.2.1. The Constraints

The penalty function method is the most widely used method in dealing with constraint conditions. The method is to add a penalty term to the fitness function so that the original constraint problem can be transformed into an unconstrained problem. However, when facing engineering problems, using the penalty function method often requires multiple adjustments and experiments, which is very time-consuming. To improve efficiency, this paper proposes an improved algorithm, demonstrated as follows:
the initial value is set as

$$\tilde{x}^{(k+1)} = \left(\tilde{x}_1^{k+1}, \tilde{x}_2^{k+1}, \ldots, \tilde{x}_n^{k+1}\right)^T \quad (1)$$

the optimal solution is

$$\bar{x}^{(k+1)} = \left(\bar{x}_1^{k+1}, \bar{x}_2^{k+1}, \ldots, \bar{x}_n^{k+1}\right)^T \quad (2)$$

if $\bar{x}^{(k+1)}$ meets the constraints and $f\left(\bar{x}^{(k+1)}\right) < f\left(x^{(k)}\right)$, then $x^{(k+1)} = \bar{x}^{(k+1)}$. Otherwise, $x^{(k+1)} = x^{(k)}$.

2.2.2. The Calculation Steps

The mathematical model after deleting redundancy is

$$\min f(x) = f\left(x_1, x_2, \cdots, x_n\right) = \sum_{j \in \Omega_1^{(K)}} \sum_{k=1}^{n} \left[v_k^{(j)}(x)\right]^2 \cdot x_k \quad (3)$$

The auxiliary is:

$$\min g(x)=\sum_{l=1}^{s}\sum_{j=1}^{J}\left\|U_{k_l}^{(j)}-U_{k_l,0}^{(j)}\right\|^2 \quad (4)$$
$$s.t. 0\le x_k\le 1/R_{k0}, k=1,2,\ldots,n$$

This model is a typical nonlinear least squares problem.

Parameters:the reference point is node 0;

the set of reachable node labels are $\Lambda=\{k_1,k_2,\cdots,k_K\}$;

the measured value of the voltage of the k_s reachable node under the j-th excitation is $U_{k_l,0}^{(j)}$ $(l=1,2,\cdots,K, j=1,2,\cdots,K)$;

the initial value of the resistance of each branch of the grounding grid is $R_i^{(0)},(i=1,2,\cdots,n)$, the allowable error is $\varepsilon_U>0$.

The detailed process is demonstrated as the following steps:

Step 1: Initialization.

The number of population individuals is set to *N*. The maximum number of iterations is *M*. The initial particle positions are $x^{(0)}=\left(x_1^{(0)},x_2^{(0)},\cdots,x_n^{(9)}\right)^T$, $x_s^{(0)}\in\left(0.001/R_s^{(0)},1/R_s^{(0)}\right)$, s = 1, 2, ⋯, n. The velocity is $v^{(0)}=\left(v_1^0,v_2^0,\ldots,v_n^0\right)$, where $k=0$;

Step 2: Evaluate the fitness of each particle in the previous step, store the current position and fitness value of each particle in each particle, and store the positions and fitness values of all individuals with the best fitness value comes along;

Step 3: Update the velocity and position to acquire $\tilde{x}^{(t+1)}=\left(\tilde{x}_1^{(t+1)},\tilde{x}_2^{(t+1)},\cdots,\tilde{x}_n^{(t+1)}\right)^T$;

Step 4: Set $\tilde{x}^{(k+1)}=\left(\tilde{x}_1^{k+1},\tilde{x}_2^{k+1},\ldots,\tilde{x}_n^{k+1}\right)^T$ as the initial value to solve least squares problem (5); $\bar{x}^{(k+1)}=\left(\bar{x}_1^{k+1},\bar{x}_2^{k+1},\ldots,\bar{x}_n^{k+1}\right)^T$

Step 5: If $\bar{x}^{(k+1)}$ meets the constraints and $f\left(\bar{x}^{(k+1)}\right)<f\left(x^{(k)}\right)$, thus $x^{(k+1)}=\bar{x}^{(k+1)}$. Otherwise, $x^{(k+1)}=x^{(k)}$;

Step 6: When the maximum time of iterations is *M*, the algorithm ends. The resistance value of each branch of the grounding grid is $\left(1/x_1^{(k+1)},1/x_2^{(k+1)},\cdots,1/x_n^{(k+1)}\right)^T$. Otherwise, go back to Step 2.

3. Simulation Analysis of Grounding Grid Fault Diagnosis

First, the standard of the corrosion degree of the grounding grid is defined, as shown in Table 1. The substation grounding grid generally uses flat steel with a cross-sectional area of 50×4mm^2 or round steel with a diameter of 20mm, and the length of each wire branch is usually 8m. The resistivity of a conductor varies with the composition of the conductor., shown in Table 2.

Table 1. *Various corrosion extents of the grounding grid conductor.*

Corrosion extent	Mild	Moderate	Severe
Multiple of resistance of grounding grid branch	0-1	2-9	>9

Table 2. *Resistivity of steels with different compositions.*

Composition	Steel	Cast Iron	Iron	Iron (pure)
Resistivity	0.1~0.2	0.57~1.14	0.0971	0.098

A schematic diagram of the experimental grounding grid with 86 branches and 49 nodes is established (Figure 2). The reachable nodes are node 2, node 7, node 11, node 17, node 26, node 37, and Node 48. The externally applied DC current excitation is 10A. The initial resistance of each branch of the grounding grid is 1Ω.

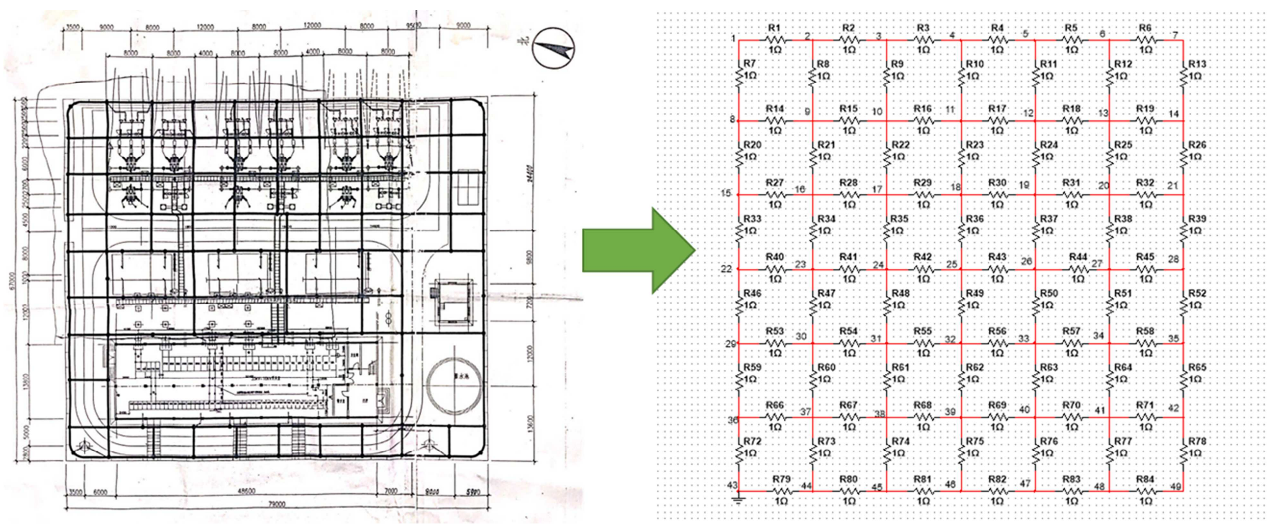

Figure 2. *Grounding grid simulation model (84 branches).*

4. Results and Analysis

4.1. Three Branches Diagnosis

Most of the actual substation grounding grid is corroded in more than one branch, hence this paper investigates the corrosion of 6 branches, respectively. First, assuming that the 15th, 16th, 48th, 54th, 55th, and 57th branches are corroded at the same time (as shown in Figure 3), and their resistance values are all Increased 4 times. The DC excitation with a size of 10A is still used, the excitation ports are rotated, and the port voltage is measured. Finally, the measurement results are imported into the diagnostic program for calculation.

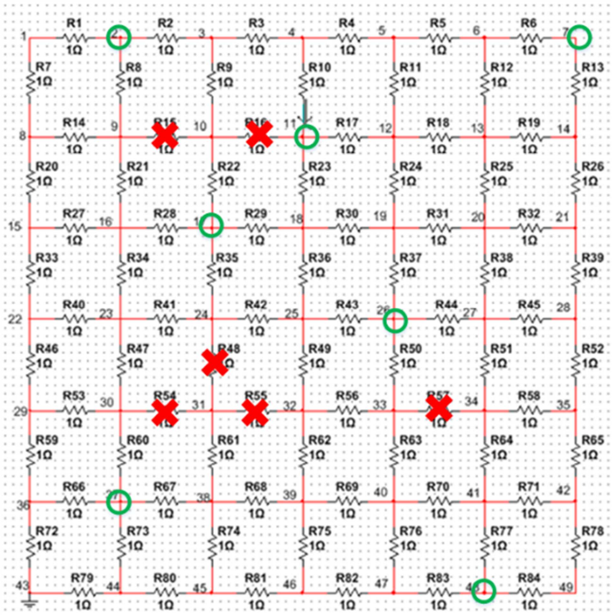

Figure 3. *Multi-branch corroded grounding grid (84 branches).*

We then substitute the measured voltage value into the compiled corrosion diagnosis program. The number of corroded branches and the extent of corrosion (i.e., the resistance increase of the corroded branch) are shown in Figure 4.

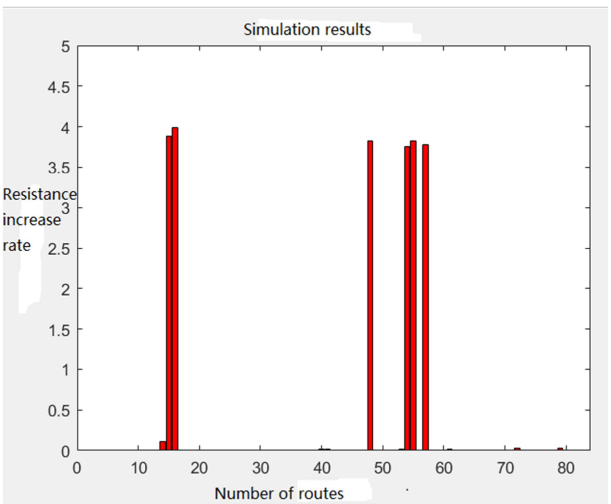

Figure 4. *Multi-branch fault diagnosis simulation.*

Figure 4 shows that the corroded branch of the grounding grid is the 15th, 16, 48, 54, 55, and 57 branches.

The corrosion resistance value and error analysis of the corroded branch are as shown in Table 3.

Table 3. *Diagnosis error of mult-branch.*

Corrosion branch number	**#15**	**#16**	**#48**	**#54**	**#55**	**#57**
Set value	5Ω	5Ω	5Ω	5Ω	5Ω	5Ω
Diagnostic result	4.88Ω	4.99Ω	4.82Ω	4.75Ω	4.82Ω	4.78Ω
Error	2.4%	0.2%	3.6%	5.0%	3.6%	4.4%

As long as the diagnosis error does not exceed 10%, the diagnosis result is considered to meet the requirements. Hence, the grounding grid diagnosis (Table 3) meets the requirements.

4.2. Ring-Shaped Branches

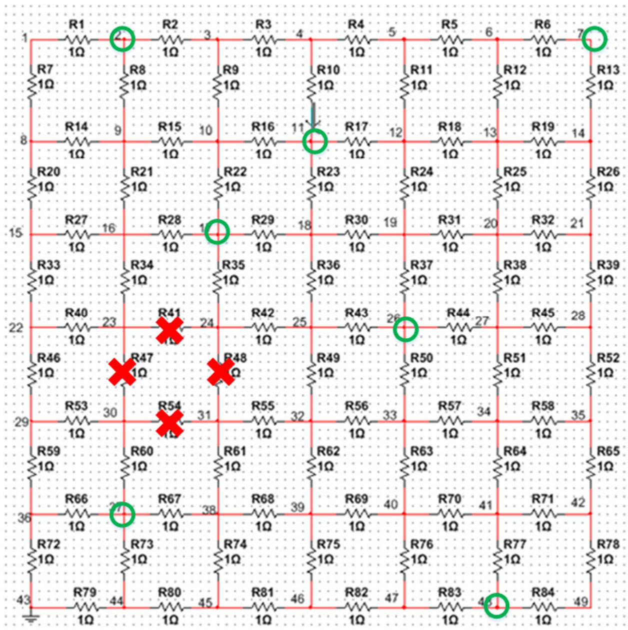

Figure 5. *Ring-shaped branches.*

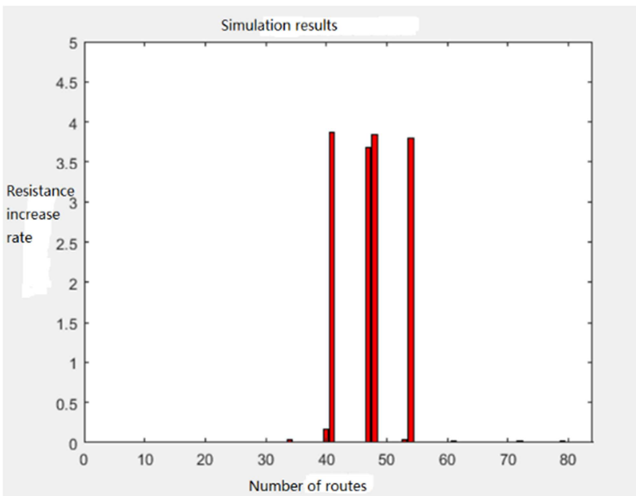

Figure 6. *Ring-shaped branches simulation.*

Assuming that the 41st, 47th, 48th, and 54th branches (forming a ring shape) are corroded at the same time (Figure 5). Their resistance values are all increased by 4 times. Other conditions are the same as before. After calculation, the number of the corroded branch and the extent of corrosion are shown in Figure 6.

Figure 6 shows that the branches where the grounding grid is corroded are the 41st, 47th, 48th, and 54th branches. The resistance value of the corroded branch and the error analysis are shown in Table 4.

Table 4. *Diagnosis error of ring-shaped branches.*

Corrosion branch number	#41	#47	#48	#54
Set value	5Ω	5Ω	5Ω	5Ω
Diagnostic result	4.87Ω	4.69Ω	4.85Ω	4.80Ω
Error	2.6%	6.2%	3.0%	4.0%

4.3. Straight-Lined Branches

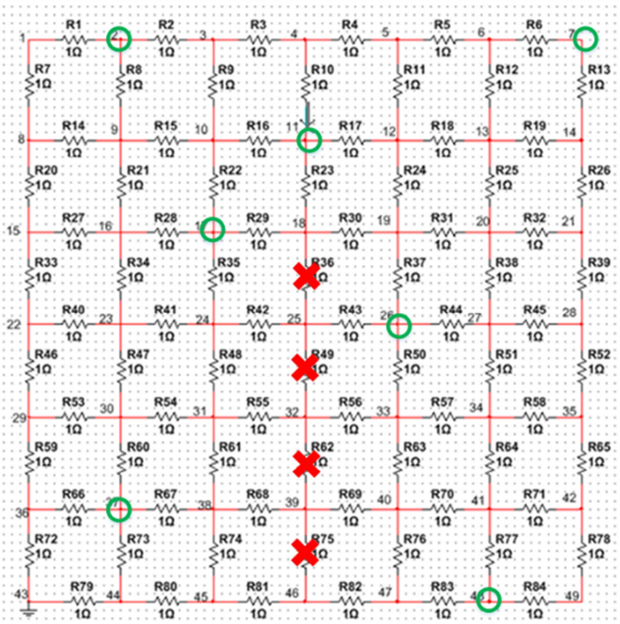

Figure 7. *Corrosion of straight-lined branches (branch 36, 49, 62, 75).*

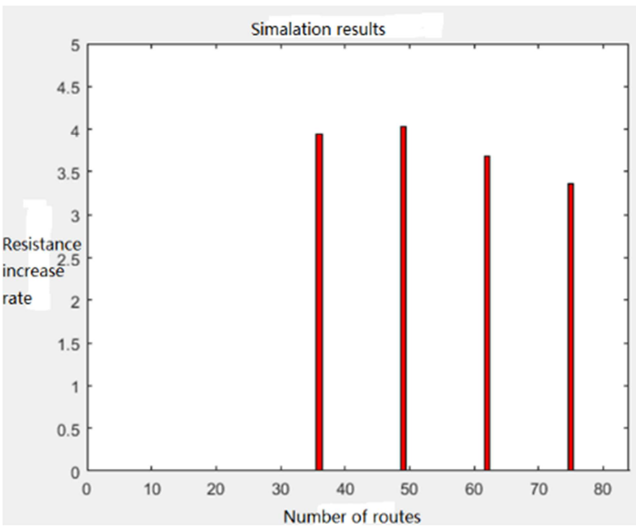

Figure 8. *Straight-lined branches simulation.*

Assuming that the 41st, 47th, 48th, and 54th branches (forming a straight line) are corroded at the same time (Figure 7). Their resistance values are all increased by 4 times. Other conditions are the same as before. After calculation, the number of the corroded branch and the extent of corrosion are shown in Figure 8.

Figure 8 shows that the branch roads where the grounding grid is corroded are 36, 49, 62, and 75 branches. The resistance value of the corroded branch and the error analysis are shown in Table 5.

Table 5. *Diagnosis error of straight-lined branches.*

Corrosion branch number	#36	#49	#62	#75
Set value	5Ω	5Ω	5Ω	5Ω
Diagnostic result	4.94Ω	5.03Ω	4.67Ω	4.35Ω
Error	1.2%	0.6%	6.6%	13%

5. Case Study

This section describes a real-world case study. First, a grounding grid model is built according to the substation grounding grid, as shown in Figure 9. The grounding grid model of the whole station includes each branch of the grounding grid and the support of the cable trench. The total station model has a total of 64 nodes, 98 branches, 8 nodes can be measured, and 28 port resistances are obtained.

Figure 9. *Grounding grid model of a 35kV substation in a certain place (for confidentiality reasons, the specific name is hidden here).*

A total of 8 grounding down-conductors and 28 port resistances are measured in the whole station. The measurement results of all port resistances are shown in Table 6.

Table 6. *Port resistance measurement (unit: milliohms).*

Port Number		Resistance	Port Number		Resistance	Port Number		Resistance
1	2	22.84	2	5	65.27	4	5	58.06
1	3	28.28	2	6	18.96	4	6	18.71
1	4	29.43	2	7	34.17	4	7	36
1	5	66.54	2	8	25.05	4	8	26.8
1	6	29.17	3	4	21.74	5	6	61.43

Port Number		Resistance	Port Number		Resistance	Port Number		Resistance
1	7	44.02	3	5	68	5	7	63.83
1	8	34.57	3	6	20.24	5	8	60.45
2	3	17.49	3	7	34.24	6	7	34.42
2	4	19.14	3	8	25.38	6	8	25.5
7	8	30.72						

Next, the port resistance results are calculated, as shown in Figure 10.

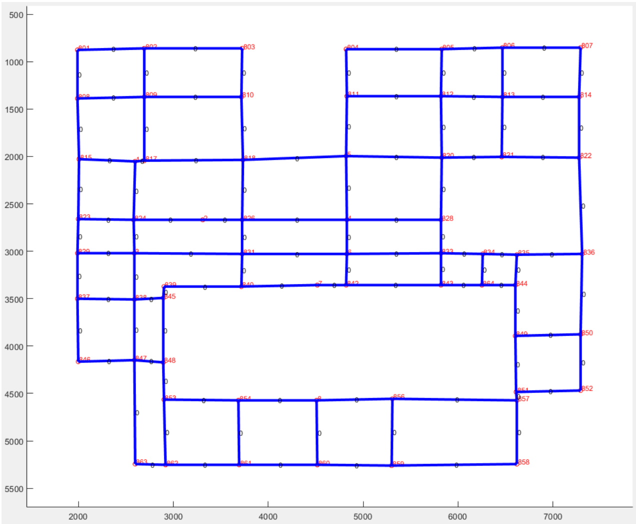

***Figure 10.** The calculation results.*

The change ratio of each branch resistance is listed in the figure, and the change rate is 0 times. The classification of the corrosion degree of grounding grid conductors are made based on the DL/T 1532-2016 (i.e., 0-1 is mild corrosion, 2-9 is moderate corrosion, and greater than 9 is severe corrosion).

From Figure 10, it can be observed that all the branch resistance change multiples are 0 times, indicating that the grounding grid has no corrosion problem. Based on the analysis results, the resistance of most of the ports is less than 50 milliohms. Hence, the diagnosis result is that the resistance of each branch increases by 0 and The overall condition of the grounding grid of this 35kV substation is good.

6. Conclusion

Corrosion is a common problem in grounding grids, which often causes serious consequences and harms the operation of the power grid. Therefore, the corrosion detection of the grounding grid is a topic that engineers have been paying close attention to. In this paper, we proposed a novel algorithm to detect the corrosion of the grounding grid. We simulate three different corrosion situations – multiple branches, ring-shaped branches, and straight-lined branches. These simulation results show that our approach provides a very efficient and useful solution.

Acknowledgements

This work was supported by an Innovation Funding of State Grid Gansu Electric Power Company, Grant No. 522711200126. We appreciate the valuable suggestions of the reviewers.

References

[1] Shadfar, Hamed, Mehrdad Ghorbani Pashakolaei, and Asghar Akbari Foroud. " Solid-state transformers: An overview of the concept, topology, and its applications in the smart grid." International Transactions on Electrical Energy Systems 31, no. 9 (2021): e12996.

[2] Hasan, Md Nazmul, Rafia Nishat Toma, Abdullah-Al Nahid, MM Manjurul Islam, and Jong-Myon Kim. "Electricity theft detection in smart grid systems: A CNN-LSTM based approach." Energies 12, no. 17 (2019): 3310.

[3] Nasir, Tehreem, Syed Sabir Hussain Bukhari, Safdar Raza, Hafiz Mudassir Munir, Muhammad Abrar, Kamran Liaquat Bhatti, Jong-Suk Ro, and Rooha Masroor. "Recent challenges and methodologies in smart grid demand side management: State-of-the-art literature review." Mathematical Problems in Engineering 2021 (2021).

[4] Bani-Ahmed, Abedalsalam, Adel Nasiri, and Igor Stamenkovic. "Foundational support systems of the smart grid: State of the art and future trends." International Journal of Smart Grid 2, no. 1 (2018): 1-12.

[5] Y. Huang, L. Hu, L. Cao, and H. Xia. Research of Grounding Grid Fault diagnosis based on differential evolution algorithm. In Proceedings of the International Conference on Power System Technology (POWERCON 2014), Chengdu, China, 20–22 October 2014, pp: 1497–1502.

[6] Y. Shao, M. Mu, B. Zhang, K. Nie, and Q. Liao. Corrosion behavior of copper-clad steel bars with unclad two-end faces for grounding grids in the red clay soil. Journal of Materials Engineering and Performance, 2017, 26 (4), 1751-1757.

[7] Sharma, Renu, and Sonali Goel. "Performance analysis of a 11.2 kWp roof top grid-connected PV system in Eastern India." Energy Reports 3 (2017): 76-84.

[8] Abdullah, Ghoname, and Hidekazu Nishimura. "Techno-Economic Performance Analysis of a 40.1 kWp Grid-Connected Photovoltaic (GCPV) System after Eight Years of Energy Generation: A Case Study for Tochigi, Japan." Sustainability 13, no. 14 (2021): 7680.

[9] X. Zhang, C. Hao, L. Chen, Y. Feng, and L. Lei. Corrosion and Protection of Metal Equipment in West Inner Mongolian Power Grid. *2020 3rd International Conference on Electron Device and Mechanical Engineering (ICEDME)*, 2020, pp: 29-32.

[10] Meliani, Meryem, Abdellah El Barkany, Ikram El Abbassi, Abdel Moumen Darcherif, and Morad Mahmoudi. "Energy management in the smart grid: State-of-the-art and future trends." International Journal of Engineering Business Management 13 (2021): 18479790211032920.

[11] Pastor, Ricardo, Wei Yang, Nuno Pinho da Silva, Sara Rodrigues, Francisco Reis, and Xue Jinhua. "Improving grid security in the presence of a high penetration of RES through optimal planning and operation of distributed energy storage devices." In 2020 IEEE 14th International Conference on Compatibility, Power Electronics and Power Engineering (CPE-POWERENG), vol. 1, pp. 370-376. IEEE, 2020.

[12] Khezri, Rahmat, and Amin Mahmoudi. "Review on the state-of-the-art multi-objective optimisation of hybrid standalone/grid-connected energy systems." IET Generation, Transmission & Distribution 14, no. 20 (2020): 4285-4300.

[13] Bajaj, Mohit, and Amit Kumar Singh. "Grid integrated renewable DG systems: A review of power quality challenges and state-of-the-art mitigation techniques." International Journal of Energy Research 44, no. 1 (2020): 26-69.

[14] W. Chen, R. Bi, J. Wang, and H. Chen. Review of Grounding Grids Corrosion Diagnosis. International Journal of Computer and Electrical Engineering, Vol. 5, No. 3, June 2013, pp: 309-312.

[15] W. Sima, X. Li, T. Yuan, and Q. Yang, “Measurement and analysis of grounding grid impulse characteristics in different soil structures,” High Voltage Technol. 2008 (07), pp: 1342–1346.

[16] Z. Fu, X, Wang, Q. Wang, X. Xu, N. Fu, and S. Qin. Advances and Challenges of Corrosion and Topology Detection of Grounding Grid. Applied Sciences, 2019.